



Hungarian University of Agriculture and Life Sciences

Mixing efficiency of paddle and screw mixers

DOI: 10.54598/004720

PhD Thesis

by

Seifeddine Garneoui

Gödöllő

2024

Doctoral school

denomination: Doctoral School of Mechanical Engineering

Science: Mechanical Engineering

Leader: Prof. Dr. Gábor Kalácska, DSc
Doctoral School of Mechanical Engineering
Hungarian University of Agriculture and Life Sciences, Gödöllő, Hungary

Supervisor: Prof. Dr. István Keppler, PhD
Institute of Technology
Hungarian University of Agriculture and Life Sciences, Gödöllő, Hungary

Co-Supervisor: Dr. habil. Péter Korzenszky, PhD
Institute of Technology
Hungarian University of Agriculture and Life Sciences, Gödöllő, Hungary

.....
Approval of the Head of Doctoral School

.....
Approval of the Supervisor(s)

CONTENTS

NOMENCLATURE AND LIST OF ABBREVIATIONS	1
1. INTRODUCTION, OBJECTIVES	2
2. MATERIALS AND METHODS	4
2.1. Image analysis of the mixing dynamics using the variance method	4
2.2. Nearest neighbor mixing index	5
2.3. Open auger screw mixer set-up	5
2.4. Paddled drum mixer set-up	6
2.5. Single-shaft paddle mixer	8
3. RESULTS	12
3.1. Introduction	12
3.2. DEM models	12
3.2.1. <i>Open auger screw mixer</i>	12
3.2.2. <i>Drum mixer</i>	13
3.2.2.1. <i>Optimal number of the drum mixer rotations</i>	15
3.2.2.2. <i>Optimal rotational mixer velocity</i>	16
3.2.3. <i>Single shaft paddle mixer</i>	17
3.2.3.1. <i>Reliability of the single shaft mixer DEM model</i>	17
3.2.3.2. <i>Effect of number of paddles</i>	18
3.2.3.3. <i>Mixing of bi-shaped particles</i>	19
4. NEW SCIENTIFIC RESULTS.....	21
4.1. Determination of the mixing efficiency of screw mixer with screw pitch length in relation to particle size	21
4.2. Optimal number of rotations of the ordinary and paddled drum mixer	22
4.3. Optimal paddled drum mixer rotational speed	21
4.4. Optimal number of paddles in a single shaft paddle mixer	21
4.5. Determination of the optimal number of rotations of the paddle mixer	21
5. CONCLUSION AND SUGGESTIONS	23
6. SUMMARY	24
7. MOST IMPORTANT PUBLICATIONS RELATED TO THE THESIS	25

NOMENCLATURE AND LIST OF ABBREVIATIONS

CoF	: Coefficient of friction [-]
$CoRF$: Coefficient of rolling friction [-]
e	: Coefficient of restitution [-]
g	: Gravity [m/s ²]
I	: Nearest neighbor mixing index [-]
M	: Mixing index [-]
N_r	: Number of rotations of the paddles [-]
N_d	: Number of rotations of the drum [-]
N_{white}	: Number of white particles [-]
N_{all}	: Total number of particles [-]
P	: Screw pitch length [mm]
σ	: Variance [-]
ϑ	: Poisson's ratio [-]
ρ	: Density [kg/m ³]
ω	: Rotational speed [rpm]
X	: Screw pitch length to average particle radius ratio [-]

DEM	: D iscrete E lement M ethod
HCP	: H exagonal C lose P acking
CoF	: C oefficient of F riction
CoRF	: C oefficient of R otational F riction
AoF	: A ngle of R epose

1. INTRODUCTION, OBJECTIVES

Mixing granular material is a common process broadly used in production and processing companies. For instance, the active components of an agricultural product in some cases are evenly distributed to ensure efficiency. The mixing procedure is of vital importance in the dosage of solid granules. The historic range of granular types and applications has led to the development of numerous apparatuses, mixing concepts, and mixing descriptions. For this reason, methods developed to mix particles cannot be applied to all mixing processes.

In various areas of engineering practices, complications arising from specific mechanical behavior of granular materials can be encountered. Under specific circumstances, granular material behaves similarly to solids (particles preserve their strength and their shape), however under other conditions the same granular material modeled earlier as solids behaves similarly to liquids, this dissemblance makes the mechanical behavior difficult to describe, yet in some case none of those models can be practical (e.g., silo discharge). Consequently, technologies used in granular materials processing (agriculture, food, pharmaceutical industries, etc.) are usually determined by experiments for a specific process. The selected method could be inappropriate, which leads to numerous technological problems. For example, in the case of drying grains, it is crucial to use the proper technology due to the expensive operating costs and high-quality requirements.

Diffusive mixing, convective mixing, and shear mixing mechanisms can be involved in mixing solid particles, which can lead to different mixture states namely: incomplete random, complete random, and perfect mixture, and even to segregation where particles do not mix completely. sampling is required to evaluate the quality of a mixture where different techniques were used either invasively or non-invasively. For the invasive method, a sampling body is thrust into the material assembly to take samples by ceasing sequentially the mixing operation or without interrupting the mixing operation. A quantitative result is obtained by physical sampling; however, the operation could change the mixture state whenever the sampling devices make contact with the particles. The other non-invasive method is to analyze snaps by way of a high-speed camera. Even though many sampling techniques are available, not enough information about the mixing process such as particle velocity, and particle coordinates could be identified.

Cundall and Strack established the discrete element method in 1979 (Cundall & Strack, 1979). This method allows us to investigate the flow of particles numerically. Over the decades, the discrete element method (DEM) was developed numerically and extended for various applications. Today, with the existence of numerical tools, the study of granule mixtures becomes more efficient, where many physical outcomes can be obtained such as particle positions in the 3D domain, particle velocity distribution, particle kinetic energy, etc. When dealing with a large bulk granular material, more computational resources are needed, however, nowadays supercomputers do exist to help solve this large material in a convenient time. In addition, using coarser particles or decreasing particle stiffness would decrease the computing time, yet either the scale-up of particle geometries or the scale-down of particle stiffness should be verified.

Mixing indexes are used to quantify the uniformity of such a mixture. The mixing index always fluctuates between 0 and 1. 0 describes the total segregation state of the mixture, and 1 defines a perfect mixture. In my research, I used the Lacey mixing index and the Nearest neighbor mixing index to quantify the conducted mixtures. The Lacey mixing index requires the division of the DEM system into cells, then it finds the mixing index based on a statistical calculation of the different types of particles. On the other hand, the Nearest neighbor mixing index quantifies the

mixture based on the position of each particle in the 3D DEM domain. As an advantage, I can find the mixing index at any desired time throughout the mixture, also many other findings could be recognized such as de-mixing, unnecessary overmixing, and optimal mixer parameters.

In the literature, there is a lack of information about the improvement of mixing in paddled mixers and screw mixers (Asachi et al., 2018) (Soni et al., 2016) (Huang & Kuo, 2014). There is not enough information on what is the optimal number of paddles that must be used to mix a certain size of particles, similarly about the size of screw pitch length and screw diameter, etc. Also there is no information on the use of a paddled drum mixer to improve the mixing homogeneity of bi-sized particles. Based on these deficiencies from the literature, I tackled the mixing of particles in screw mixers and paddled mixers to improve the mixing homogeneity by finding the optimal parameters that should be used and to support solving these open questions.

The goal of my research is to improve the homogeneity of particles by selecting the proper mixing apparatus, mixing parameters, and mixing time as over-mixing is costly and might result in segregation. The list of objectives set to achieve are the following:

- To find the optimal screw pitch dimension as a function of particle radius in a screw auger mixer.
- To improve the mixing effectiveness of particles in a rotating drum mixer by adding paddles in the middle of the mixer. Identify the optimal number of rotations of the drum when mixing mono-sized and bi-sized particles, in which the mixing homogeneity is at its maximum.
- To build a single shaft paddles mixer and analyze its mixing effectiveness.
- To find the optimal rotational speed of a paddled drum mixer in terms of mixing uniformity.
- To find the optimal number of paddles in a single-shaft paddle mixer in terms of mixing uniformity.
- To find the optimal number of rotations of a single-shaft paddle mixer in terms of mixing uniformity.

2. MATERIALS AND METHODS

This chapter encompasses a detailed account of the materials, methodologies, and equipment utilized in conducting the experimental measurements essential for achieving the research objectives.

2.1. Image analysis of the mixing dynamics using the variance method

To check the reliability of the DEM models, I have used a high-speed camera to take snaps along the mixture from the top of the single shaft paddled mixer (Fig.1). This would give an insight into the structure of the mixture from the top layer and then I divided each structure into several cells and then applied the particles variance method to quantify these mixing states of particles.

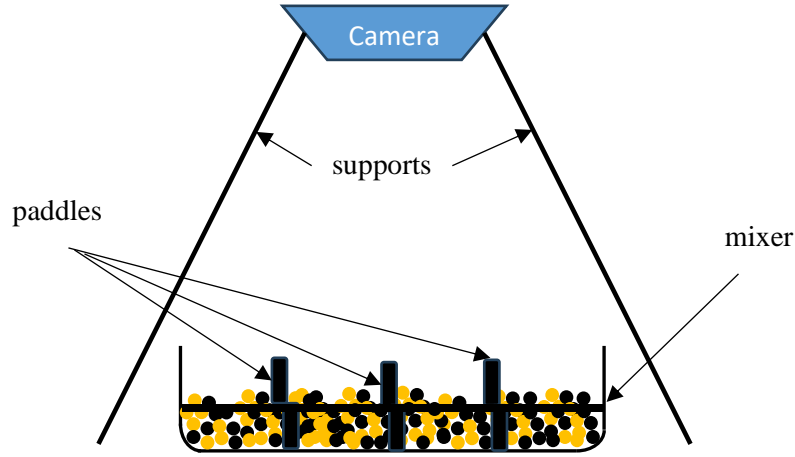


Fig. 1. Description of the setup used to capture particle distribution by images

The variance method is a useful technique to quantify the distribution of particles from a 2D image (Liu et al., 2015). A grid must be assigned to the bed region to get a certain number of cells, and the quality of the mixture is quantified by the concentration variance of the system.

$$\sigma^2 = \frac{1}{n-1} \sum_{i=1}^n (C_i - C)^2. \quad (1)$$

Assume mixing a bi-component material distinguished by color white and black, then the concentration of a particular component in cell i is calculated by:

$$C_i = \frac{\text{number of black particles}}{\text{number of black particles} + \text{number of white particles}}. \quad (2)$$

And C is the average value calculated as following:

$$C = \frac{1}{n} \sum_{i=1}^n C_i. \quad (3)$$

σ^2 equals 0.5 if the particles are segregated, and σ^2 approaches 0 if decent homogeneity of particles is attained.

I used this quantification method to plot the different mixing curves and find the difference between the real experiment and the DEM simulation in a rotational drum mixer.

2.2. Nearest neighbor mixing index

This mixing rate is calculated using the coordinates of all types of particles in the DEM domain (Gorter et al., 2010). The 12 nearest particles to each particle are identified by iteration, then the equation (47) is applied to find the mixing rate of the concerned element, and similarly for all other particles, finally a mean value is calculated of the mixing rates found of each particle to describe the homogeneity level of the whole mixed material bed.

$$M = \frac{1}{N} \sum_{i=1}^N \frac{2 \times n_{diff}}{n_{nb}}. \quad (4)$$

N , n_{diff} , n_{nb} are the total number of particles, the number of particles different in type, and the number of neighboring particles, respectively.

A slight modification could be introduced in case of using unequal quantities of particle types are used. For instance, a material bed composed of 1000 particles of type *A* and 2000 particles of type *B*. In this case, the perfect mixture of particle *i* is attained only if 4 type *A* particles and 8 type *B* particles are found as the nearest particles.

For this method, I created a Java script that finds the rate by reading the coordinates from a CSV file because it is smooth and practical. In the appendix, I presented a script of this method.

2.3. Open auger screw mixer set-up

A hopper base screw mixer was studied in this work. The mixer has an upper diameter of 100 mm, a base diameter of 30 mm, and a length of 250 mm, all including 5 mm wall thickness. A schematic of the conic base mixer is presented in Figure 1. A side-by-side particle initial configuration is used. The shape of the particle we used to mix is described in Fig 3.

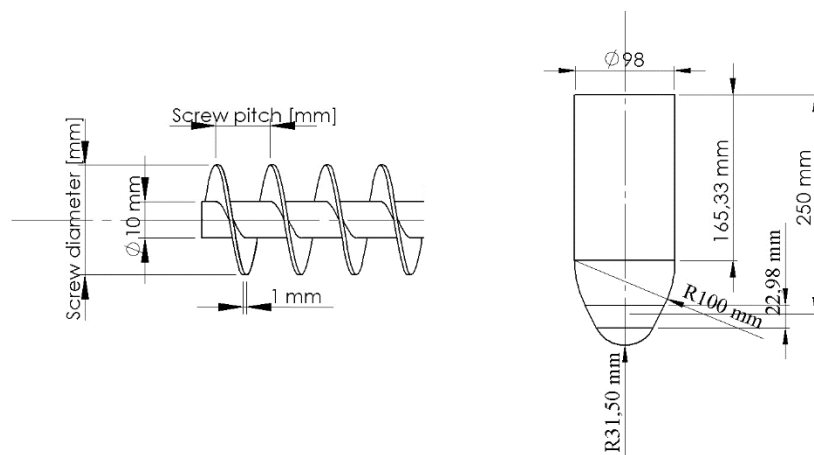


Fig. 2. Geometry of the mixer and screw geometrical parameters studied.

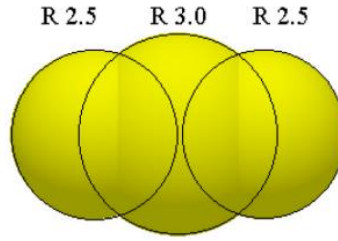


Fig. 3. Geometry of the mixer and screw geometrical parameters studied.

I investigated the impact of the screw pitch length described in Figure 1 and I used the same mechanical properties listed in Table 1.

The simulation scenarios with the related parameters conducted are listed in Table 2. The time-step magnitude is set at 20 % of the Rayleigh time-step and the elapsed simulation time is 60 s.

Table 1. Micro-mechanical parameters used in the drum mixer simulations (Keppler et al., 2016)

Parameters	Particle (wheat)	Mixer wall (steel)
Poisson ratio ν	0.4	0.3
Shear modulus G (Pa)	$3.58 \cdot 10^9$	$8 \cdot 10^8$
Density ρ (kg/m ³)	1460	7500
Coefficient of restitution e	0.5	0.6
Coefficient of friction CoF	0.3	0.25
Coefficient of rolling friction $CoRF$	0.01	0.01

Table 2. List of the conducted numerical simulations for the screw mixer

Runs	Initial configuration of particles	Screw direction of rotation	Screw pitch length (mm)	Screw diameter (mm)	Screw rpm
Run 1	Side-by-side	clockwise	10	10	60
Run 2	Side-by-side	clockwise	20	10	60
Run 3	Side-by-side	clockwise	30	10	60
Run 4	Side-by-side	clockwise	40	10	60
Run 5	Side-by-side	clockwise	50	10	60

2.4. Paddled drum mixer set-up

I used a literature reference to create a DEM model of a cylindrical drum mixer assigned with acrylic material having a diameter of 280 mm and a width of 140 mm, to find the reliability by comparing my results to that of Li et al., (Li et al., 2009). The mixer was filled and maintained at 75 % filling fraction by volume for all simulations with spherical glass beads, segregation state was set before mixing by generating two groups of particles from separate inlets on the top of the mixer separated by a cross-sectional splitter placed in the middle of the mixer to study the

homogeneity of particles mixture from an inhomogeneous mixture state, knowing that particles filling time is 1 s. The diameters of the two types of particles used are 10 mm and 5 mm. A 1:1 filling volume ratio was maintained for all simulation cases inside the drum. After complete filling of particles, the splitter was removed and the material bed settled down until it reached a stationary state in the mixer under the influence of gravity for 1 s time, followed by the rotation of the mixer vessel for 75 s time to ensure the mixing uniformity to reach its highest rate.

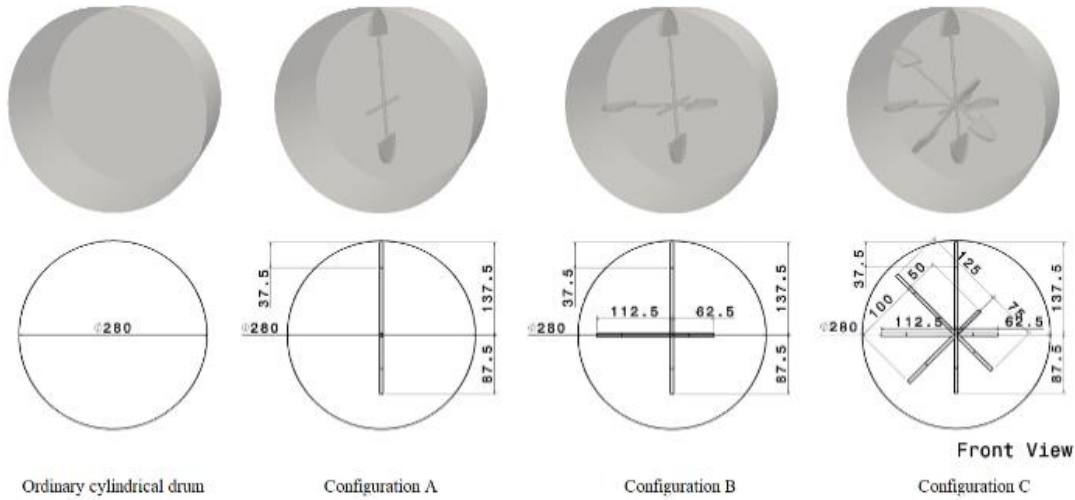


Fig. 4. Set-ups of the cylindrical drum used in simulations

I used the micro-mechanical properties provided by Yanjie et al., (Li et al., 2009) displayed in Table 3 to define the mixer wall and particle materials and describe particle-particle and particle-wall interactions, and the DEM timestep that I used for all the simulations is 40 % of the Rayleigh timestep.

Table 3. Micro-mechanical parameters used in the drum mixer simulations (Li et al., 2009)

Properties	Particles (glass spheres)	Mixer wall (acrylic sheet)	Particle-wall
Density, ρ (kg/m ³)	2700	1800	-
Young's modulus, E (Pa)	10^7	10^7	-
Coefficient of restitution, e	0.67	-	0.67
Poisson's ratio, ν	0.22	0.35	-
Coefficient of friction, CoR	0.95	-	0.8
Coefficient of rotational friction, $CoRF$	0.05	0.05	-

In the middle of the mixer frame, I added uneven paddles, and I examined the impact of these paddles on the mixture homogeneity. The drawings of the paddle mixer configuration are shown in Fig. 4. The radius of the blade of each paddle has the shape of a semi-cylinder and its radius is 50 mm.

The simulation scenarios are described in Table 4. Initially, simulation cases 1 to 4 and 5 to 11 were conducted to check the efficacy of the different mixer designs in terms of mixture uniformity.

Eventually, the mixer speed was varied only for the finest mixer set-up in terms of mixing efficacy. Simulation cases 5 to 11 tackled the impact of mixer rotational velocity (configuration C) on the mixture homogeneity.

Table 4. Design of numerical experiments of the rotational drum mixer

Simulation	Mixer set-up	Material bed	Mixer rotational speed
Run 1 to 4	Ordinary drum	Bi-disperse	8 rpm
	Configuration A		
	Configuration B		
	Configuration C		
Run 5 to 11	Configuration C	Bi-disperse	16 rpm
			24 rpm
			32 rpm
			40 rpm
			48 rpm
			60 rpm
			70 rpm

2.5. Single-shaft paddle mixer

I built a single-shaft paddle mixer as a mixer prototype that could be used to improve the mixing technologies. The mixer is described in Fig. 5. The apparatus has a frame, two supports to hold the frame, a mixing rotor, and an electric controllable-speed motor. The different parts of the mixer were 3D printed using PLA material. The mixing rotor is changeable which allows changing the number and shape of paddles if needed.

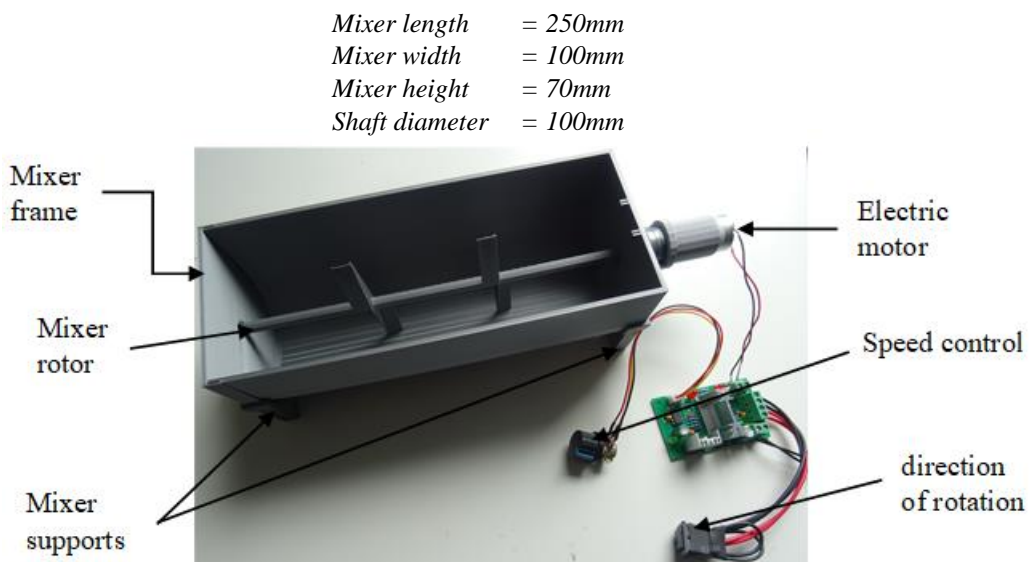


Fig. 5. Set-up of the single-shaft paddle mixer

The mixer was filled with corn grains, and these grains were partitioned equally in two types distinguished by color and an initial segregation state was set before mixing. A high-resolution camera was placed above the mixer to capture high-quality snaps during the mixing process. These snaps would give an insight into the mixture quality and compare the distribution of the particles

from the top layer to that of the developed DEM models for correlation check. After the filling of particles, the motor was turned on, the paddles were rotated in the clockwise direction and grains were moved in the mixer for 40 s mixing time until a steady state was reached.

I used the values of the grain particle density, Young's modulus, and particle-particle coefficient of restitution found by using the pendulum collision experiment from the study of Montellano (C. González-Montellano, 2012), while for the particle-particle coefficient of restitution, I used the drop experiment by releasing one particle without an initial velocity towards a plate having the same mixer material. A high-speed camera is used to capture the position of a particle before and after bouncing. The particle will make a vertical trajectory H_2 after bouncing and then the coefficient is calculated according to the principle of kinematics as follows:

$$e = -\frac{v_1}{u_1} = \sqrt{\frac{H_2}{H_1}} \quad (5)$$

In this experiment, the particle-wall coefficient of restitution found is 0.505. This result is the average value of 50 replications by releasing two distinct corns from 200 mm and 300 mm heights (H_1 in Fig. 6).

The corn grain has a complex shape, modeling this grain with a simple sphere is unrealistic and results will diverge, therefore I employed the multi-sphere approach in LIGGGHTS to thoroughly mimic the real shape of a corn particle.

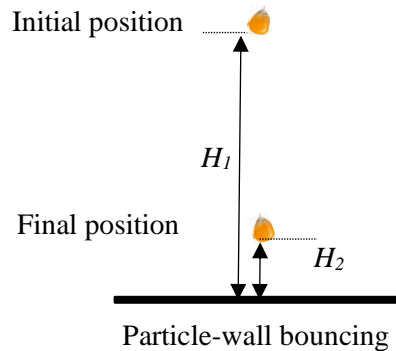


Fig. 6. Measurement illustration of the particle-wall coefficient of restitution

I used a clump of 5 spheres as described in Fig. 7. I found that this shape is the best to represent the corn grain by comparing the magnitudes of the repose angles found from DEM and real experiments shown in Fig. 8.

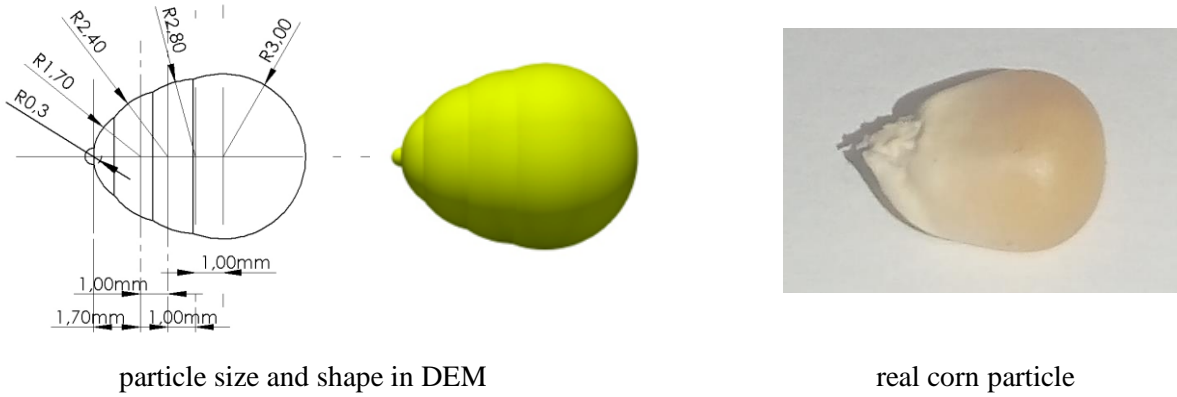


Fig. 7. DEM particle shape and size of a corn grain

To measure the coefficients of static and rolling frictions, I conducted the storehouse unloading experiment. A roofless box having the dimensions of 75mm×75mm×75mm is fixed on a flat base. The box was loaded with 1000 grains, and then one side of the box was pulled out, as a result, the loaded material will freely slide out of the box in a way that it will form a slope. Calibration experiments using DEM experiments were performed to find the optimal values. Figure 7 shows the comparison of real experiments and DEM simulations.

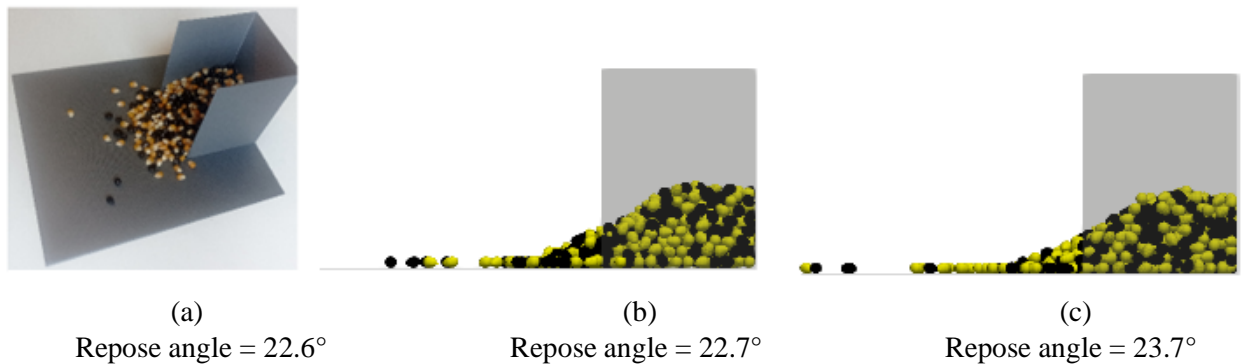


Fig. 8. Slope angles calculated by filling 1000 grains: (a) real test (b) numerical test using real value of E and 20 % Rayleigh timestep (c) numerical essay using $E=5 \cdot 10^6$ Pa and 20 % Rayleigh timestep

As the material is opaque, I used a protractor to find the slope angle and compare it to numerical results. The slope angles obtained by the real experiment and the numerical simulation with smaller values of Young's moduli were 22.6° and 23.7°, respectively, which closely matched.

The timestep used is 20 % of the Rayleigh timestep in all the simulations.

Table 5. Micro-mechanical parameters used in the single-shaft mixer simulations

Properties	Particles (corn)	wall	Particle-wall
Density, ρ (kg/m ³)	1163.3	1250	-
Young's modulus, E (MPa)	$5 \cdot 10^6$	$5 \cdot 10^6$	-
Coefficient of restitution, e	0.25	-	0.505
Poisson's ratio, ν	0.4		0.235
Coefficient of friction, CoF	0.6	-	0.7
Coefficient of rolling friction, $CoRF$	0.05	-	0.05

The list of conducted simulations with the configurations set are listed in Table 6.

Table 6. Listed of simulations conducted for the single-shaft paddle mixer

Run	Paddles' shape	Number of paddles	Initial filling type	Particles shape
1	B	2	Side-wise	Mono-shaped
2	A	2	Side-wise	Mono-shaped
3	A	3	Side-wise	Mono-shaped
4	A	4	Side-wise	Mono-shaped
5	A	5	Side-wise	Mono-shaped
6	A	6	Side-wise	Mono-shaped
7	A	7	Side-wise	Mono-shaped
8	A	5	Top-bottom	Mono-shaped
9	A	6	Top-bottom	Mono-shaped
10	A	7	Top-bottom	Mono-shaped
11	A	5	Top-bottom	Bi-shaped
12	A	5	Top-bottom	Bi-shaped

3. RESULTS

In this chapter, the crucial findings derived from the experimentation are outlined along with their corresponding discussions.

3.1. Introduction

All the results obtained from the DEM simulations are evaluated quantitatively using the mathematical models described in the methods chapter to calculate the mixing rates, thus finding the influential factors on the quality of mixed particles.

Various types of mixers were utilized: open auger screw mixer, drum mixer, and a single shaft mixer are utilized to mix a bi-component solid particle. Important findings are discussed and parameters for optimal mixing are given for each type of mixer used.

3.2. DEM models

For each DEM model, contact information, material properties, and boundary conditions are specified, then the DEM model is executed. The simulations are carried out using EDEM[®] or LIGGGHTS[®] programs. In the case of using the latter, generated data are opened with PARAVIEW[®] to visualize results.

3.2.1. Open auger screw mixer

Simulations in Table 5 were carried out using a screw having the following pitch lengths: 10mm, 20mm, 30mm, 40mm, and 50mm, while the screw diameter and screw speed maintained constant at 3.5mm and 60rpm, respectively. I calculated the average mixing index for an elapsed simulation time $t=20s$ (Figure 45).

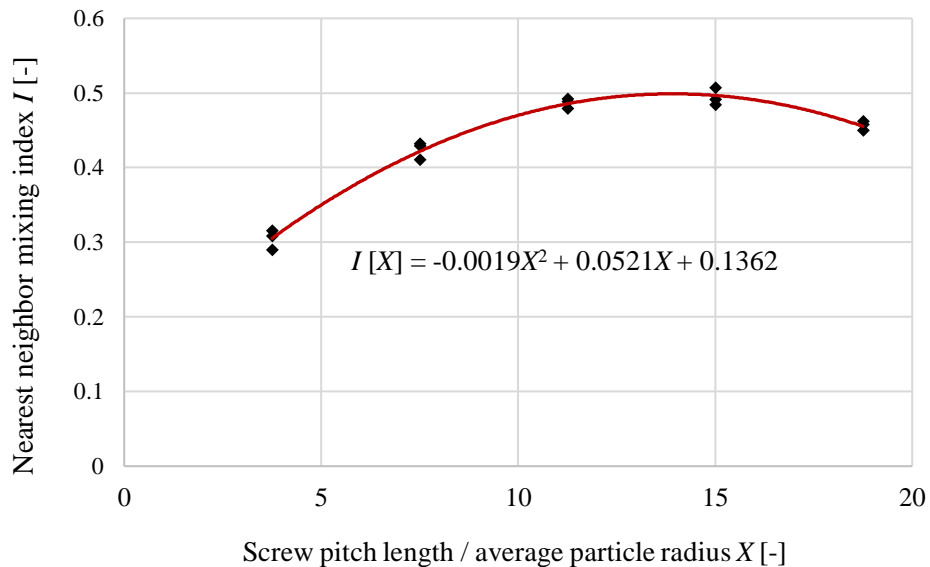


Figure 1. Optimal mixing index in function of screw pitch length to average particle radius ratio

I found that the best mixing effectiveness in terms of mixing uniformity in the screw mixer based on the screw pitch length and particle average radius rapport can be approximated using the following polynomial equation.

$$I(X) = -0.0019X^2 + 0.05210 X + 0.1362 \quad (6)$$

Where: $I(X)$: Nearest neighbor mixing index [-], X : Screw pitch length to average particle radius ratio [-]. The equation is valid on the condition that X ranges from 3.75 to 18.75, the coefficient of determination is 0.985.

3.2.2. Drum mixer

To check the reliability of the drum mixer DEM model, I conducted three simulations with the same parameters set used by Soni et al., (Soni et al., 2016) and I compared the distribution of particles by taking snapshots from the side of the mixer wall to the real experiments (Fig. 9).

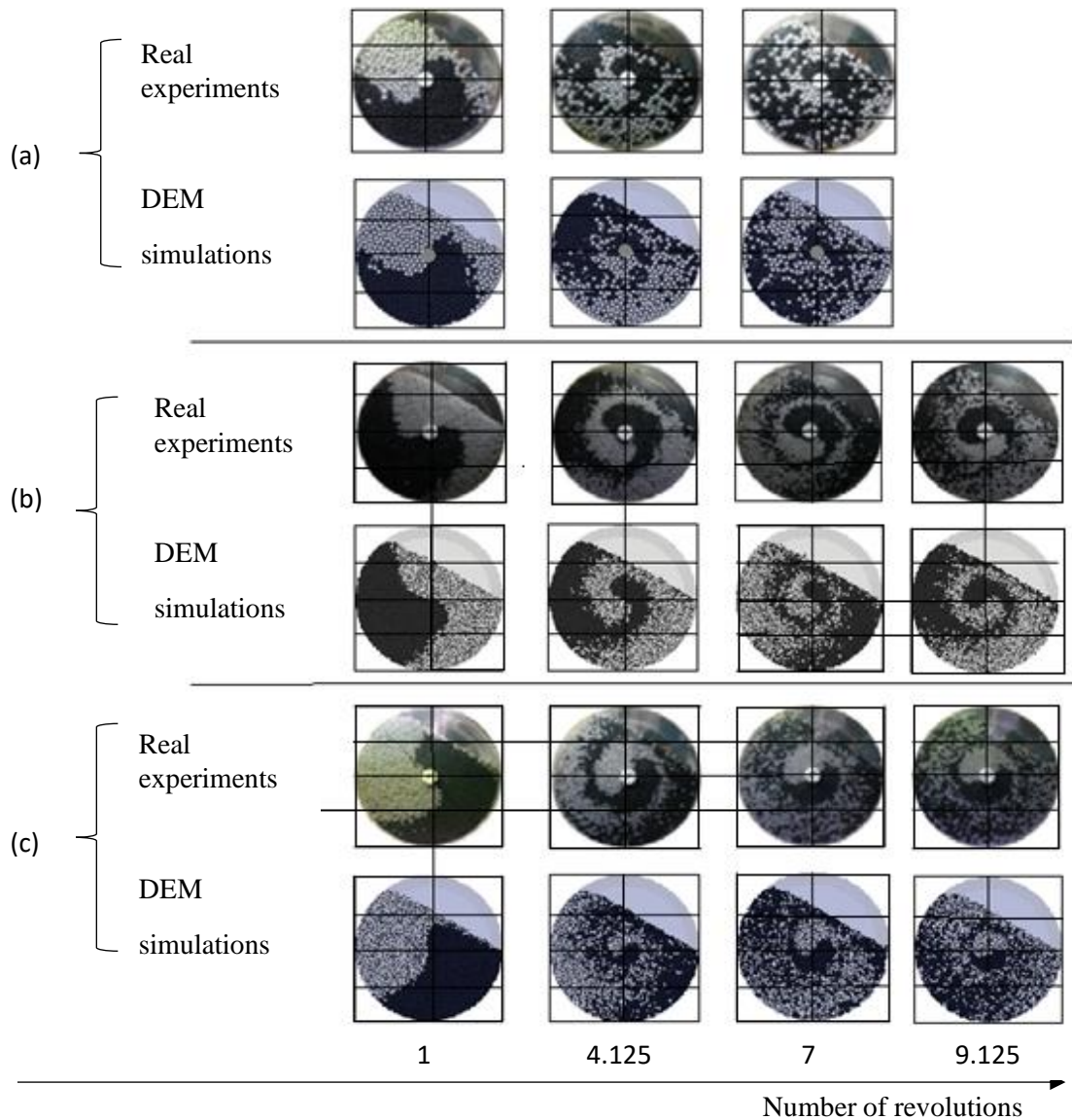


Fig. 9. Mixing states of real experiments obtained from literature and numerical simulations at 4rpm drum rotational speed (a) drum rotational speed 4 rpm and particle diameter 10 mm (b) drum rotational speed 4 rpm and particle diameter 5 mm (c) drum rotational speed 8 rpm and particle diameter 5 mm

I applied the system concentration variance method described in section 2.1 in the previous chapter to examine the difference between results quantitatively. I used the same grid for all results with

8 cells to find the difference in the number of particles. The average difference in the system concentration variance between the experiments and the DEM simulations is the following:

- 9% using 10mm particles' diameter at a 4rpm drum rotational speed (Fig. 10)
- 2.5% using 5mm particles' diameter at a 4rpm drum rotational speed (Fig. 11)
- 4.5% using 5mm particles' diameter at an 8rpm drum rotational speed (Fig. 12)

As a result, the concentration variance found proves that the DEM model has an acceptable level of accuracy and could be used to study the mixing of particles.

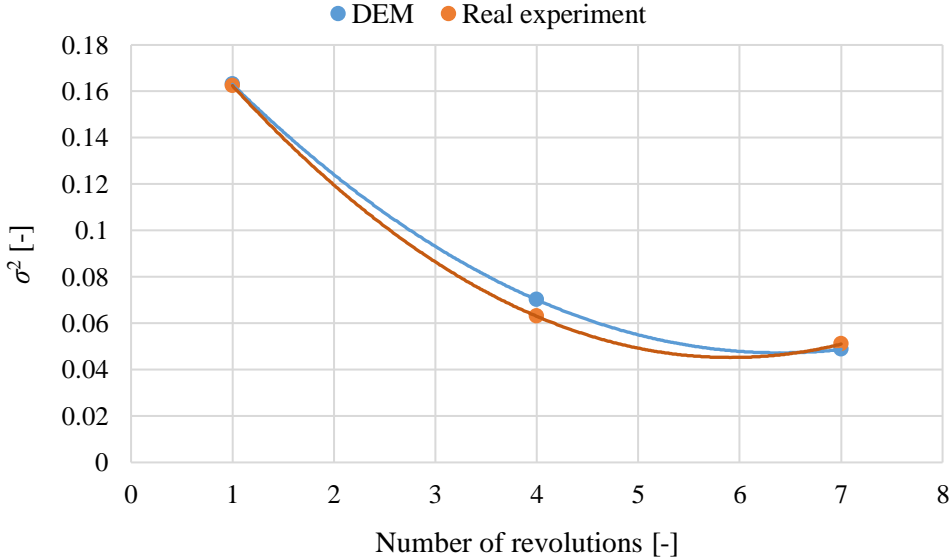


Fig. 10. Concentration variance of particles using 10mm particles' diameter at 4rpm drum rotational speed

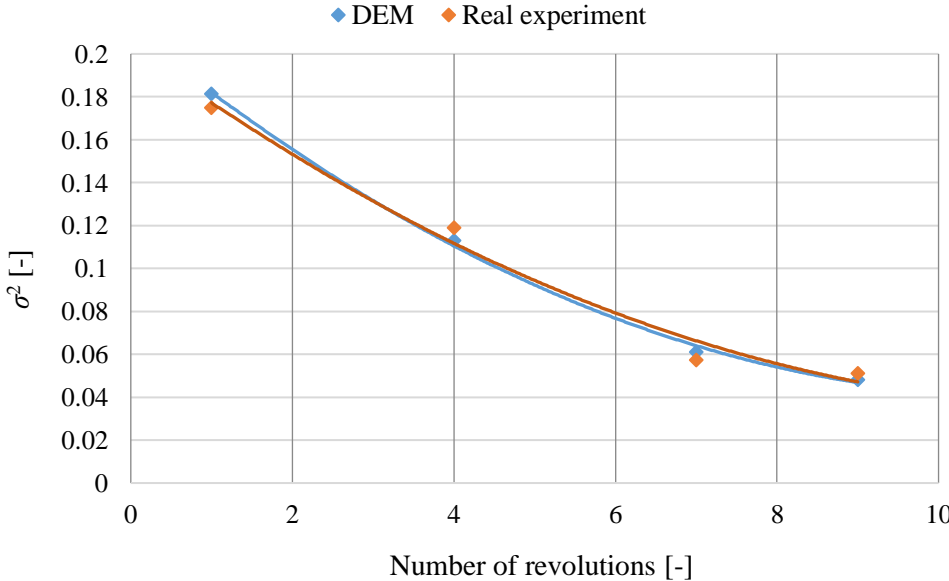


Fig. 11. Concentration variance of particles using 5mm particles' diameter at 4rpm drum rotational speed

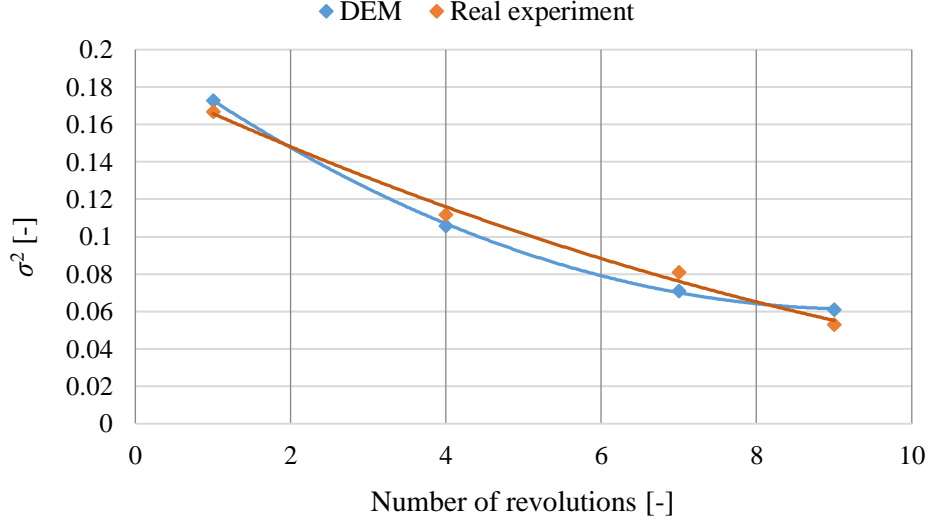


Fig. 12. Concentration variance of particles using 5mm particles' diameter at 8rpm drum rotational speed

3.2.2.1. Optimal number of the drum mixer rotations

In this part, I tackled the mixing of unequally sized particles. In this case, three mechanisms should be deemed: convection, diffusion, and segregation. The first two mechanisms sustain mixing. Convective mixing is also known as macro mixing which helps the granular material bed to turn around the mixer frame from one side to another and diffusive mixing involves the random displacement of a particle within a material bed, letting particles change their position relative to one another. However, segregation (the opposite term of mixing) disfavors mixing due to the so-called stratification phenomenon, as smaller particles tend to slip down the material bed through the voids between larger particles. This has been elucidated due to the uneven displacement of larger particles against smaller particles during mixing (Yongzhi Zhao, 2008). Because a segregation mechanism could arise, then an appropriate mixing time should be selected to avoid insignificant over-mixing.

Simulation cases 1 to 4 described in Table 4 were conducted. Fig. 13 shows how the homogeneity index of the binary system evolves during mixing time for the different drum set-ups. A mixing to de-mixing transition is perceived from the curve wherein the highest mixing degree is obtained at around 40 seconds of mixing time. Mixing beyond this time causes de-mixing.

Using regression analysis, I obtained the following polynomial equation:

$$I(N_d) = -10^{-6}N_d^3 - 0.0002N_d^2 + 0.012N_d + 0.011. \quad (7)$$

Where: $I(N_d)$: Nearest neighbor mixing index [-], N_d : Number of rotations of the drum mixer [-]. This result is valid for ordinary drum mixer and all paddled mixer configurations from 7 to 75 rotations of the mixer. The coefficient of determination is 0.9092.

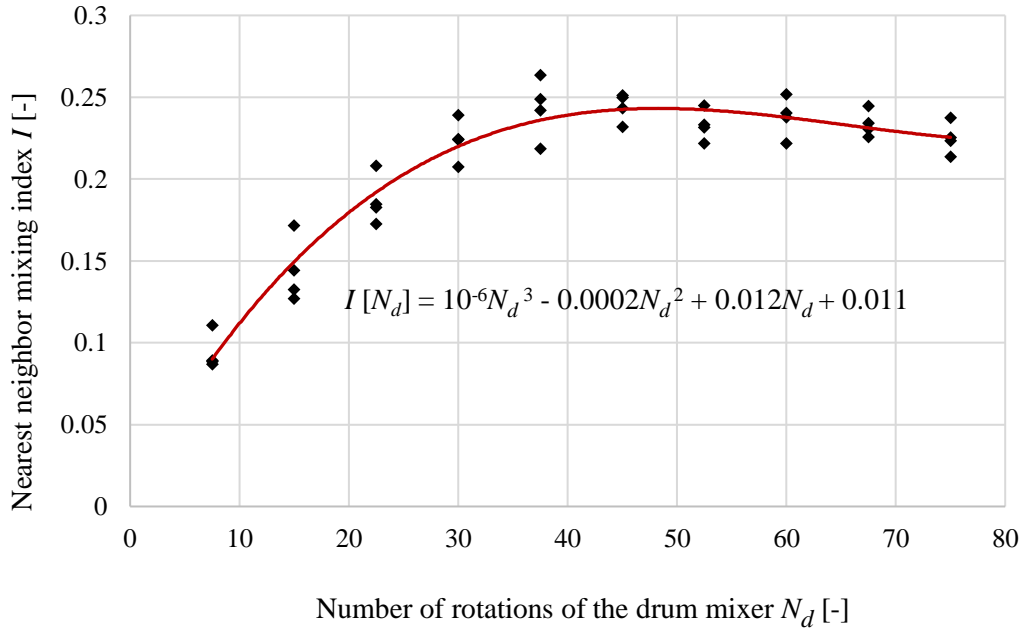


Fig. 13. Variation in the overall mixing index of bi-disperse (diameters are 10mm and 5mm) particles for different rotations of the paddled drum mixer

3.2.2.2. Optimal rotational mixer velocity

According to results obtained in the previous sub-sections, it is obvious that the mixing of bi-disperse particles is rather complex and requires enhancement. For this purpose, I furthered simulations by gradually increasing the drum speed from 8 rpm to 16 rpm, 24 rpm, 32 rpm, 40 rpm, 48 rpm, 60 rpm, and 80 rpm. Related homogeneity indices along the mixing process were calculated as average for an elapsed mixing time of 80 s and illustrated in Fig. 14.

By increasing the drum speed, the mixture quality improves, whereas increasing the drum speed above 60rpm is inefficient as confirmed at 70rpm and 80rpm.

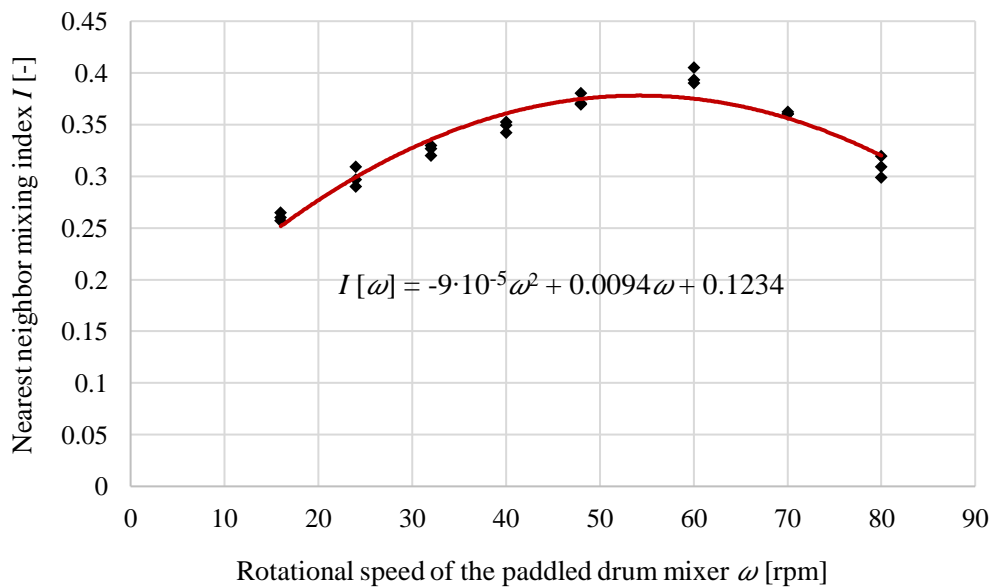


Fig. 14. Optimal number of rotations of the drum mixer for 80s fixed mixing time

I found that in a paddled drum mixer the mixing uniformity increases until it reaches the peak based on an optimal number of rotations of the drum mixer, while further increasing the number of rotations of the drum will result in a deficiency of the mixing efficiency.

Using regression analysis, I obtained the following polynomial equation:

$$I(\omega) = -9 \cdot 10^{-5} \omega^2 + 0.0094 \omega + 0.1234. \quad (8)$$

Where: $I(\omega)$: Nearest neighbor mixing index [-], ω : rotational speed of the drum mixer [rpm].

The equation is valid on the condition that n ranges from 15 to 80 rpm. The coefficient of determination is 0.916.

3.2.3. Single shaft paddle mixer

In this part, I investigated the effects of particle shape and the number of paddles on the mixing uniformity. I used bi-colored corn grains as solid particles. To calculate the static friction, rolling friction, and the coefficient of restitution, I performed box discharging technique. The coordinates-based mixing rate so-called nearest neighbor index was employed to quantitatively examine the different mixing rates along the mixing period according to the variables: filling type and paddles number.

3.2.3.1. Reliability of the single shaft mixer DEM model

By analyzing the surface layer of the material in the mixer, I could identify the similarity amount. I used a high-speed camera to take snaps from the top of the mixer without interrupting the operation, then I analyzed the captured snaps. I divided each capture into 8 cells (Fig. 15), and the same for the DEM model. I examined the effectiveness of the DEM model by checking on the one hand the distribution similarity of yellow particles in each cell. I found an average similarity of 95 % when analyzing snaps captured every 5 s which proves the reliability of our DEM models.

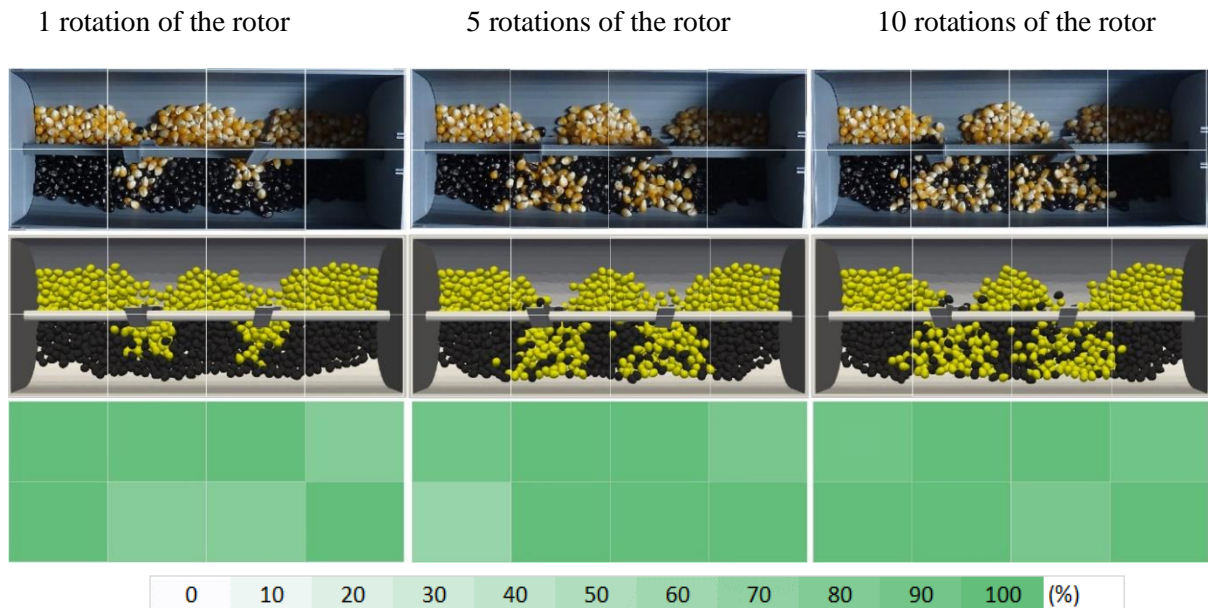


Fig. 15. comparison of particle distribution in the mixer with the DEM simulation

On the other hand, I varied the capture speed as follows: 1 image per second, 1 image per 2 seconds, 1 image per 3 seconds, 1 image per 4 s, and 1 image per 5 s. Applying the quantification of the

image analysis described in section 2.1 based on particles' variance, the regression lines obtained are shown in Fig. 16. The average variance between the two curves is around 5.1 % which confirms the reliability of the DEM model.

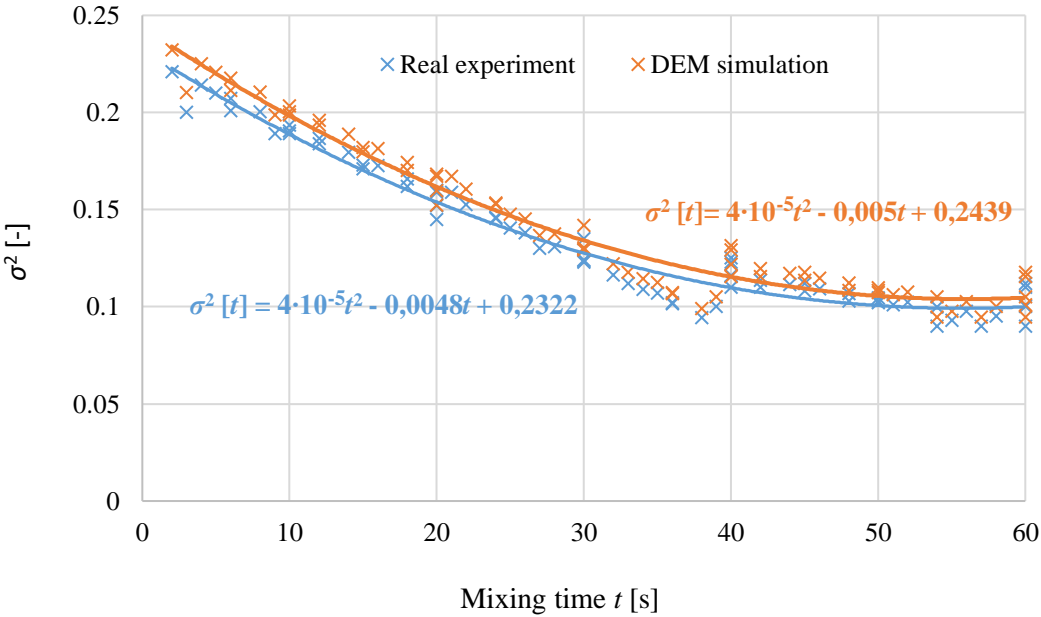


Fig. 16. Comparison of mixing curves determined by particle concentration variance

3.2.3.2. *Effect of number of paddles*

The second set of simulations tackled the effect of number of paddles on the mixing rate. The distance between every two paddles and between the mixer wall and the paddle are all identical. The best mixing index is achieved when using more paddles (Fig. 17) while using more than 5 paddles is unnecessary as the difference between 5 and 6 paddles on the mixing index is trivial (around 0.9 % difference as average). The calculated mixing index for every number of paddles used is the average in 90 s mixing time.

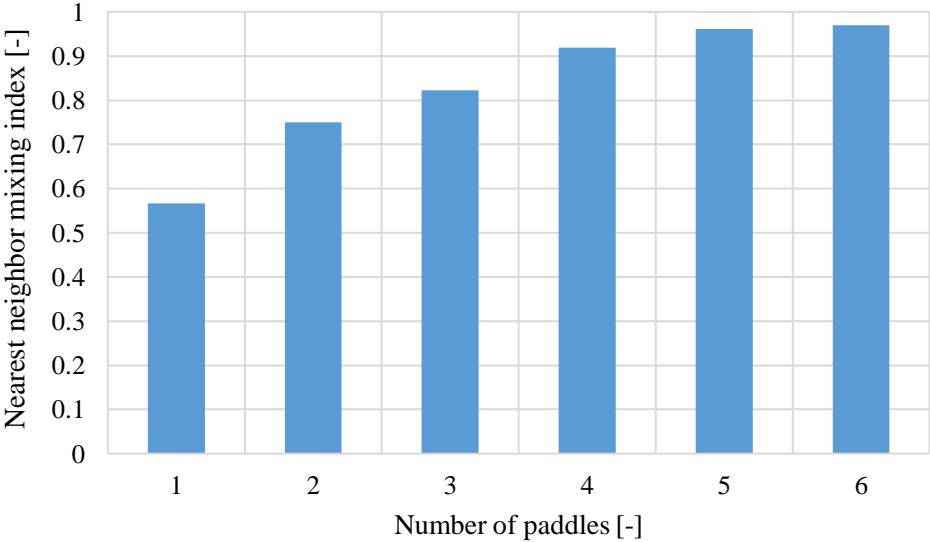


Fig. 17. Effect of paddles number on the mixing efficiency

The improvement of the mixing rate is achieved because of the elimination of dead zones when using more paddles in the mixer. Fig. 18 shows a comparison of the dead regions formed in the mixer when using 2 paddles and 5 paddles after 10 rotations of the paddles (the mixing paddles' rotational speed is fixed at 10rpm).

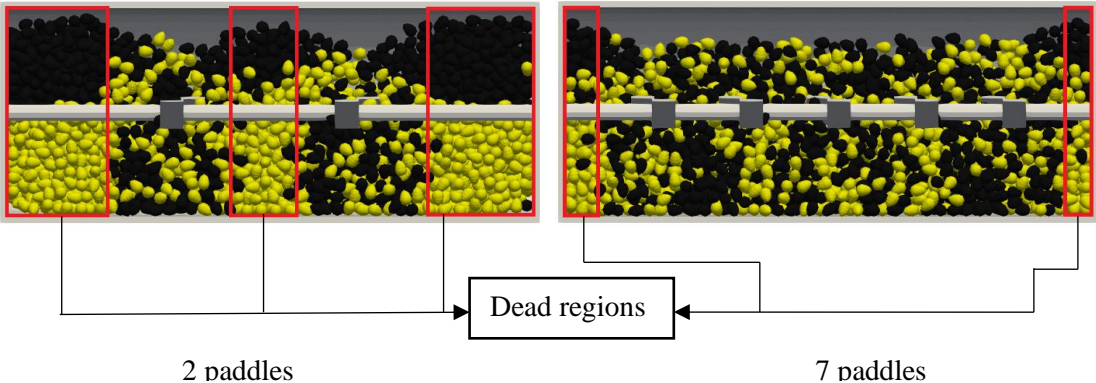


Fig. 18. Size of dead regions after 25s mixing time at 10 rpm of the paddles.

3.2.3.3. *Mixing of bi-shaped particles*

In this part, I studied the mixing of bi-shaped. I used the shapes illustrated with the dimensions in Fig. 19. The rotational speed of the paddles was kept constant at 10 rpm. I found that the mixing efficiency of those bi-shaped particles is reached at 2.5 rotations.

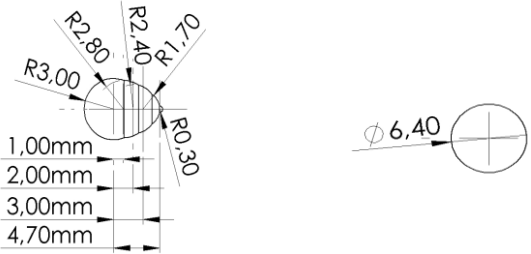


Fig. 2 . shape and dimensions of particles mixed

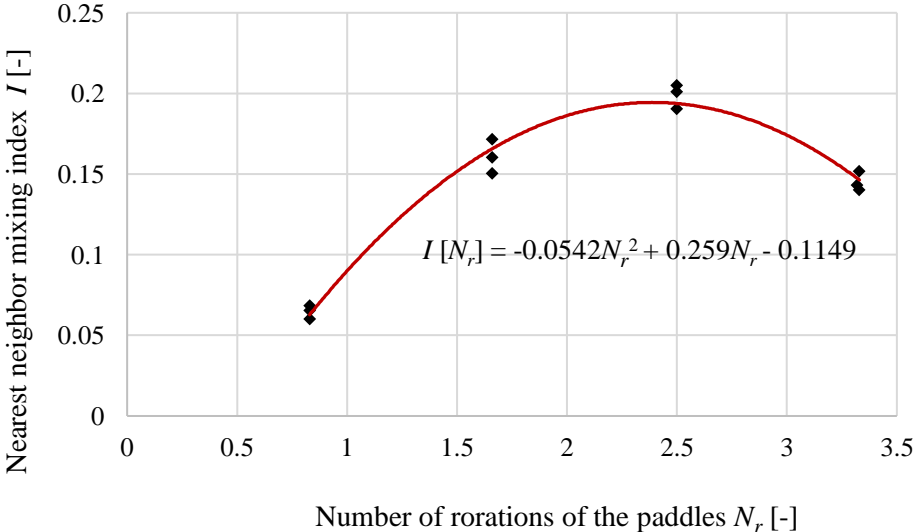


Fig. 20 . Optimal number of rotations of the paddles when mixing bi-shaped particles

There is an optimal paddle rotation number when mixing bi-shaped particles in the single-shaft paddle mixer to reach the best mixture uniformity while overrunning this number of rotations leads to particle segregation. The mixing efficiency can be approximated using the following polynomial equation:

$$I(N_r) = -0.1149 + 0.2590 N_r - 0.05424 N_r^2 \quad (9)$$

Where: $I(N_r)$: Nearest neighbor mixing index [-], N_r : Number of rotations of the paddles [-]. The equation is valid for 0.7 to 3.5 rotations of paddles.-The coefficient of determination is 0.979.

4. NEW SCIENTIFIC RESULTS

4.1. Determination of the mixing efficiency of screw mixer with screw pitch length in relation to particle size

I found that the best mixing effectiveness in terms of mixing uniformity in the screw mixer based on the screw pitch length and particle average radius rapport can be approximated using the following polynomial equation.

$$I(X) = -0.0019X^2 + 0.05210 X + 0.1362 \quad (10)$$

Where: $I(X)$: Nearest neighbor mixing index [-], X : Screw pitch length to average particle radius ratio [-]. The equation is valid on the condition that X ranges from 3.75 to 18.75, the coefficient of determination is 0.985.

4.2. Optimal number of rotations of the ordinary and paddled drum mixer

I have identified while mixing a bi-disperse material bed, a mixing to de-mixing transition can be perceived from the curves of the mixing indices for all types of paddled drum mixers. Mixing beyond the optimal number of rotations causes de-mixing for all configurations, independently of the shape and spatial configuration of the paddles.

Using regression analysis, I obtained the following polynomial equation:

$$I(N_d) = -10^{-6}N_d^3 - 0.0002N_d^2 + 0.012N_d + 0.011. \quad (11)$$

Where: $I(N_d)$: Nearest neighbor mixing index [-], N_d : Number of rotations of the drum mixer [-]. This result is valid for ordinary drum mixer and all paddled mixer configurations from 7 to 75 rotations of the mixer. The coefficient of determination is 0.9092.

4.3. Optimal paddled drum mixer rotational speed

I found that in a paddled drum mixer the mixing uniformity of the bi-disperse material increases until it reaches the peak based on an optimal number of rotations of the drum mixer, while further increasing the number of rotations of the drum will result in a deficiency of the mixing efficiency. Using regression analysis, I obtained the following polynomial equation:

$$I(\omega) = -9 \cdot 10^{-5}\omega^2 + 0.0094\omega + 0.1234. \quad (12)$$

Where: $I(\omega)$: Nearest neighbor mixing index [-], ω : rotational speed of the drum mixer [rpm]. The equation is valid on the condition that ω ranges from 15 to 80 rpm. The coefficient of determination is 0.916.

4.4. Optimal number of paddles in a single shaft paddle mixer

I determined that the mixing index increases during the mixing of mono-shaped particles in the single shaft paddle mixer when the number of paddles increases, while there is no reason to increase the number of paddles above 5 as the mixing index doesn't increase using more

paddles. This phenomenon is related to the dead zone arising around the moving paddles, as by increasing the number of paddles, the possible size of dead zones is decreasing.

4.5. Determination of the optimal number of rotations of the paddle mixer

I found that there is an optimal paddle rotation number when mixing bi-shaped particles in the single-shaft paddle mixer to reach the best mixture uniformity while overrunning this number of rotations led to particle segregation. The mixing efficiency can be approximated using the following polynomial equation:

$$I(N_r) = -0.1149 + 0.2590 N_r - 0.05424 N_r^2 \quad (13)$$

Where: $I(N_r)$: Nearest neighbor mixing index [-], N_r : Number of rotations of the paddles [-]. The equation is valid for 0.7 to 3.5 rotations of paddles.-The coefficient of determination is 0.979.

5. CONCLUSION AND SUGGESTIONS

The conclusions of the study concerning mixing enhancement of wheat particles in a hopper bottom screw mixer are the following:

- I found that when the ratio screw pitch length to particle average ratio is 15, the mixing efficiency reaches the maximum.

To enhance both mono-disperse and bi-disperse particles in a cylindrical drum mixer, various number of paddles were unevenly installed in the middle of the mixer. The performance of the paddles' configurations was investigated by using discrete element simulations, followed by quantitative analysis. The following conclusions can be drawn from the simulation results:

- When mixing a bi-disperse material bed at 60 rpm fixed rotational speed, a mixing to de-mixing transition is obtained. Mixing beyond the optimal number of rotations which is 45 causes de-mixing for all configurations, independently of the shape and spatial configuration of the paddles. An improvement of the mixture uniformity of 10.5 % is achieved at 45 rotations compared to 52.5 rotations of the mixer.
- At 10 rpm fixed rotational speed, the mixing uniformity improved by 26.5 % at 2.5 rotations compared to 3.25 rotations when mixing bi-shaped particles: clumps of 5 spheres and regular spheres.

As for suggestions, this study revealed that mixing a bi-disperse material at a high filling level of the cylindrical drum is rather complex and challenging. Therefore, novel designs of the drum mixer could be effective in tackling this issue. Furthermore, the same methodology could be utilized to investigate the effect of more particle size ratios and particle shapes on the mixture quality in the drum mixer.

The following conclusions can be drawn from my study on the single-shaft paddle mixer:

- Results showed that using more paddles increases the mixing homogeneity, because less dead zones will be formed.
- The optimal number of rotations of the paddles at 10 rpm fixed rotational speed of the paddles to achieve the best homogeneity state when mixing bi-shaped particles is 2.5 rotations, while mixing above this number of rotations of the paddles leads to segregation because the mixing index decreased by 27 % when mixing the particles at 3.33 rotations of the paddles.

This study demonstrates that the grain drop, and box discharging experiments are effective in determining the different micro-mechanical properties. In addition, the multi-sphere approach to represent a complex shape of grains is adequate in the DEM code.

6. SUMMARY

MIXING EFFICIENCY OF PADDLE AND SCREW MIXERS

In the case of a mixing process of solid particles such as the mixing of pharmaceutical powders and chemical products, the main concern is that the different particles should be evenly distributed within the granular assembly. This homogeneous distribution of solid elements could only be achieved if an effective mixing operation is carried out. Therefore, adequate parameters should be set to avoid additional costs and time loss.

My study aims to build reliable DEM models that can be used in real processes to investigate the flow of particles around the mixer and to select the optimal parameters based on several factors such as particle shape, particle type, etc.

I used the Discrete Element Method to describe mixing by mechanical means. This method is powerful and has been developed by many scientists and programmers in recent years. I used EDEM® at first in a small part then I furthered conducting simulations using LIGGGHTS® in a big part of our work because of its flexibility and the possibility to use KIFÜ's Hungarian Supercomputer to run models in a short time. In our models, I decreased the simulation time by reducing the value of Young's modulus by comparing the slope angle results. I proved that Young's modulus magnitude could be decreased to 5×10^6 Pa in a paddle mixer to significantly decrease the computational time without altering the actual result however, it is not always the case when using other types of mixers or particles (it must be always checked).

I employed mixing indices to quantify the different mixtures. This would let us know the uniformity value which ranges from 0 to 1. I coded the nearest neighbor mixing index in Java to simplify the calculation, and also to have more accurate results because this method relies on the coordinates of particles inside of the mixer.

I found that the geometry of the drum mixer has an impact on the uniformity of particles. By installing paddles, the uniformity has been improved. In addition, there is an optimal rotational speed of the drum mixer to obtain the best mixture uniformity.

A better mixture homogeneity is obtained when adding horizontal paddles to the screw in a crew mixer because it would let particles move around the mixer wall. I also revealed that there is an optimal screw pitch length, and increasing its length would adversely impact the homogeneity of particles.

Modeling corn grains using the multi-sphere approach in the single-shaft paddle mixer gives acceptable results. I found that the type of particle filling influenced the homogeneity of particles, when filling one type of particle then filling the other type on top of it gave the highest uniformity rate, also there is an optimal number of rotations of the paddles when mixing bi-shaped particles.

7. MOST IMPORTANT PUBLICATIONS RELATED TO THE THESIS

Refereed papers in foreign languages:

1. Garneoui, S., Korzenszky, P., & Keppler, I. (2023). Enhancement of the mixture quality of corn grains in a single-shaft paddle mixer using DEM simulations. *Journal of Mechanical Science and Technology*, 37(3), 1365–1373. <https://doi.org/10.1007/s12206-023-0223-1>
2. Talafha, S.M., Oldal, I., & Garneoui, S. (2022). Study the particle size impact on the mechanical behaviour of granular material by discrete element method. *FME Transactions*, 50(3), 473–483. <https://doi.org/10.5937/fme2203473t>
3. Garneoui, S., Korzenszky, P, & Keppler, I (2022): Mixing Enhancement of Mono-Disperse and Bi-Disperse Particles in a Cylindrical Drum Mixer Using Discrete Element Simulations. (2022). *Tehnicki Vjesnik - Technical Gazette*, 29(3), 752-758. <https://doi.org/10.17559/tv-20210303201549>
4. Garneoui, S., Keppler, I., Korzenszky, P., & Talafha, S.M, (2021): Numerical study on the impact of particles filling pattern and screw parameters on the mixing uniformity of wheat grains in a screw mixer. *Applied and Computational Mechanics*, 15 (2), 123-<http://dx.doi.org/10.24132/acm.2021.689>
5. Garneoui, S., Keppler, I., & Korzenszky, P (2020): Numerical Assessment of a Static Mixer Design for Mixing Free Flowing Granular Materials Using the Discrete Element Method. *Journal of Mechanical Engineering and Technology (JET)*, 11 (2), 23-36. <https://jet.utem.edu.my/jet/article/view/5972>
6. Garneoui, S., Keppler, I., & Korzenszky, P (2020): Mixing Enhancement of Wheat Granules in a Hopper Bottom Lab-Scale Mixer Using Discrete Element Simulations. *FME Transactions*, 48 (4), 868-873. <http://dx.doi.org/10.5937/fme2004868G>
7. Garneoui, S., Keppler, I., & Korxenszky P (2022): Impact of screw pitch length on the mixture quality of grains in a small-scale silo apparatus. *Mechanical Engineering Letters: R and D: Research and Development*, 23, 4-12. <http://dx.doi.org/10.24132/acm.2021.689>